J. Biochem. **140**, 561–571 (2006)
doi:10.1093/jb/mvj189

Characterization of Heme-Coordinating Histidyl Residues of Cytochrome b_5 Based on the Reactivity with Diethylpyrocarbonate: A Mechanism for the Opening of Axial Imidazole Rings

Nobuyuki Nakanishi[1], Fusako Takeuchi[1], Hidetsugu Okamoto[1], Atsuo Tamura[1], Hiroshi Hori[2] and Motonari Tsubaki[1,3,*]

[1]Department of Molecular Science and Material Engineering, Graduate School of Science and Technology, Kobe University, Rokkodai-cho, Nada-ku, Kobe, Hyogo 657-8501; [2]Division of Bioengineering, Department of Mechanical Science and Bioengineering, Graduate School of Engineering Science, Osaka University, Machikaneyama-cho, Toyonaka, Osaka 560-8531; and [3]CREST, JST

Received August 1, 2006; accepted August 30, 2006

We investigated the reactivity of heme-coordinating imidazole with diethylpyrocarbonate using a soluble domain of cytochrome b_5. Analyses with various spectroscopic methods including MALDI-TOF-MS indicated that two axial His residues (His44 and His68) of cytochrome b_5 were protected from the modification by several factors, *i.e.*, limited steric exposure of the axial imidazole to the solvent, the Fe-$N_{\varepsilon 2}$ coordination bond, and protonation of the $N_{\delta 1}$ position by forming a hydrogen bond with its immediate surroundings. However, once *N*-carbethoxylation at the $N_{\varepsilon 2}$ position of the axial His residues occurred with a higher concentration of diethylpyrocarbonate, displacement of heme prosthetic group from the protein moiety continued. Simultaneously, it facilitated the second *N*-carbethoxylation to take place at the $N_{\varepsilon 1}$ position of the same imidazole ring, leading to a bis-*N*-carbethoxylated derivative and further to a ring-opened derivative. A similar mechanism seemed in operation for one non-axial His residue (His85), in which the $N_{\delta 1}$ atom works as a hydrogen acceptor in a strong hydrogen-bond and the other $N_{\varepsilon 2}$ atom is in a protonated form, resulting in a formation of the ring-opened derivative upon treatment with a higher concentration of diethylpyrocarbonate. These results suggested that the use of diethylpyrocarbonate for MALDI-TOF-MS analysis might provide a unique method to characterize the protonation state of His residues and the strength of their hydrogen-bondings at the active site of enzymes.

Key words: cytochrome b_5, diethylpyrocarbonate, histidyl residue, MALDI-TOF, *N*-carbethoxylation.

Abbreviations: DEPC, diethylpyrocarbonate; LMWb5, the hydrophilic domain of human cytochrome b_5; MALDI-TOF, matrix-assisted laser desorption/ionization-time of flight; VHA-Mb, a six-coordinated myoglobin mutant, in which triple mutations (H64V/V68H/H93A) were introduced in porcine myoglobin to adopt six-coordination of the heme prosthetic group.

Histidine (His) residues are known to participate in a very wide range of functions in different proteins. The imidazole side chain of His residues has two nitrogen atoms ($N_{\delta 1}$ and $N_{\varepsilon 2}$) with different properties; one donates only one electron to the imidazole ring so it has a free lone pair and is basic; while the other is bound to a hydrogen atom and donates its lone pair to the ring and, therefore, is slightly acidic. These properties of the imidazole side chain are exploited in different ways in many proteins. Hemoproteins contain a heme prosthetic group, either covalently or non-covalently bound to the protein itself, and are found in diverse roles such as transport of dioxygen (hemoglobin and myoglobin), signal transduction (heme-containing sensors), catalysis (peroxidases), active membrane transport (respiratory cytochromes), and electron transfer (cytochromes). The iron atom in the heme prosthetic group being coordinated by mostly $N_{\varepsilon 2}$ atom[1] of the imidazole ring is the center for such diverse reactivities and is capable of undergoing oxidation and reduction. The other nitrogen atom ($N_{\delta 1}$) is protonated at a physiological pH and may function to form a hydrogen-bond network around the heme moiety to facilitate such various activities at the heme center.

During a series of our studies on cytochrome b_{561} residing in the chromaffin vesicle membranes and participating in the transmembrane electron transfer from cytosolic ascorbate to intravesicular monodehydroascorbate radical to supply electron equivalents to intravesicular copper-containing monooxygenases (*7–10*), we began to focus

*To whom correspondence should be addressed. Tel/Fax: +81-78-803-6582, E-mail: mtsubaki@kobe-u.ac.jp

[1] The majority of hemoproteins having His residues as an axial ligand are known to make the coordination to heme iron with their $N_{\varepsilon 2}$ atoms. Only a few exceptions to have an Fe-$N_{\delta 1}$ bond are known, such as the *c*-type low-spin heme-I in the tetra-heme cytochorme c_{554} from the bacterium *Nitrosomonas europaea* (*1*) and the Met65His mutant of the heme domain of cellobiose dehydrogenase (*2*).

our attention on the reactivity of the heme axial His residues with diethylpyrocarbonate (DEPC), a well-known chemical modification reagent for His residues (*11*). This reagent attacks a deprotonated nitrogen atom of an imidazole group to form *N*-carbethoxylated derivatives. In the present study, we exploited a soluble domain of human cytochrome b_5 as a suitable model to study the DEPC-modification of heme-coordinating imidazole groups. Previous studies showed that DEPC-treatment of bovine cytochrome b_5 showed a significant release of a heme prosthetic group from the protein moiety due to a rupture of the iron-imidazole cooridination bond (*12, 13*). We utilized various spectroscopic techniques (including MALDI-TOF-MS, EPR, ^{1}H-NMR, and visible absorption spectroscopy) to clarify the structure around the heme-cooridinating imidazole groups of cytochrome b_5 and the mechanism of their *N*-carbethoxylation reactions.

EXPERIMENTAL PROCEDURES

Plasmid Construction, Expression, and Purification of Soluble Somain of Human Cytochrome b_5—The gene coding for a soluble domain (1–99 amino acid residues) of human cytochrome b_5 in pIN3/b5/2E1/OR plasmid (*14, 15*) was subcloned into pCWori vector (*16*) in the following manner. PCR products amplified using the forward primer carrying an *Nde*I site and the reverse primer carrying a *Hin*dIII site were digested with *Nde*I and *Hin*dIII followed by a ligation into the pCWori vector. *Escherichia coli* strain BL-21(DE3)pLysS, which has the T7 RNA polymerase gene in its chromosome under the control of a lacUV5 promoter, was transformed with the pCWori vector containing the soluble domain of human cytochrome b_5. T7 RNA polymerase could then be expressed by the addition of IPTG to the medium. The original coding sequence was confirmed with a DNA sequencer (PRISM 310 Genetic Analyzer, ABI).

The soluble domain of human cytochrome b_5 (LMWb5) was produced by growing the transformed cells at 37°C in TB (12 g/liter of tryptone, 24 g/liter yeast extract, 4 ml/liter glycerol, 23.1 g/liter KH_2PO_4, and 125.4 g/liter K_2HPO_4) in the presence of ampicillin (100 μg/liter). Induction of protein expression was achieved by the addition of 10 μM (final) IPTG when the cells had grown to an O.D. of 1.0–1.5 at 600 nm. Then, the incubation temperature was lowered to 20°C. Cells were harvested 48 h after the addition of IPTG and were frozen in liquid nitrogen and stored at –80°C overnight. The thawed cells were mixed with a lysis buffer (10 mM sodium phosphate buffer pH 8.0 containing 1.0 mM EDTA) and disrupted by the treatment with lysozyme (1 mg/ml) followed by sonication. The disrupted cells were centrifuged at 11,000 rpm at 4°C. The supernatant was saved as a crude extract.

Purification of LMWb5 was conducted as follows. The crude extract was loaded onto a column of DEAE-Sepharose CL-6B previously equilibrated with 10 mM Tris-HCl, 1 mM EDTA (pH 8.0) buffer. The LMWb5 was adsorbed in the column as a reddish band. The column was washed with the same buffer containing 50 mM NaSCN. The adsorbed LMWb5 was eluted by a linear gradient of NaSCN concentration from 50 to 300 mM in the same buffer. The main fraction was collected, diluted with the same buffer without NaSCN and loaded onto a second DEAE-Sepharose CL-6B column previously equilibrated with 10 mM sodium phosphate buffer (pH 7.0) containing 1 mM EDTA. The column was washed with the same buffer containing 100 mM NaCl. The adsorbed LMWb5 was eluted by a linear gradient of NaCl concentration from 100 to 300 mM in the same buffer. Main fractions were collected based on the SDS-PAGE analysis (12% gel) and were concentrated to about 1 ml using Amicon concentrator and Microcon YM-10 (Amicon). The concentrated LMWb5 was then subjected onto a gel-filtration chromatography with Sephacryl S-200HR (Amersham Bioscience) previously equilibrated with 50 mM potassium phosphate buffer (pH 7.0) containing 1 mM EDTA and 100 mM NaCl. The main fractions were collected based on the analysis of SDS-PAGE, concentrated, and were subjected onto a second (and/or the third) gel-filtration chromatography with Superdex 75 (Amersham Bioscience) previously equilibrated with 50 mM potassium phosphate buffer (pH 7.0) containing100 mM NaCl. Fractions that showed a single protein band on SDS-PAGE were pooled together and concentrated, gel-filtrated against 50 mM potassium phosphate buffer (pH 7.0) with PD-10 mini-column (Amersham Bioscience).

Modification of LMWb5 with Diethylpyrocarbonate—Concentrated LMWb5 solution in oxidized state was diluted with 50 mM potassium-phosphate buffer (pH 6.5) to an appropriate concentration. The sample was, then, treated with various concentrations of DEPC for 30 min, as previously described (*7, 9*). The DEPC-treated samples were gel-filtered through a PD-10 column equilibrated with 50 mM potassium-phosphate buffer (pH 6.5) to remove unreacted DEPC. The DEPC-treated LMWb5 was then analyzed for the reactivity with AsA using a Shimadzu UV-2400PC spectrophotometer. Finally, the sample was fully reduced with sodium dithionite and its absorption spectrum was recorded to check the integrity of the heme moiety.

EPR Spectroscopy—Oxidized LMWb5 samples (either control or DEPC-treated in the oxidized form) in 50 mM potassium-phosphate buffer (pH 7.0) were concentrated to about 230 μM with a 50-ml Amicon concentrator fitted with a membrane filter (Millipore PTTK04310; pore size 30,000 NMWL). The concentrated samples were introduced into EPR tubes and frozen in liquid nitrogen (77 K). EPR measurements were carried out at X-band (9.23 GHz) microwave frequency using a Varian E-12 EPR spectrometer with 100-kHz field modulation. An Oxford flow cryostat (ESR-900) (from 5 to 20 K) was used. The microwave frequency was calibrated with a microwave frequency counter (Takeda Riken Co., Ltd., Model TR5212). The strength of the magnetic field was determined with an NMR field meter (ECHO Electronics Co., Ltd., Model EFM 2000AX). The accuracy of the *g*-values was approximately ±0.01.

NMR Spectroscopy—^{1}H-NMR spectra were measured at 298 K on a Bruker DMX-750 spectrometer with a repetition time of 4.6 s. LMWb5 samples were dissolved in 50 mM deuterated potassium-phosphate buffer (pH 7.0) at a final protein concentration of either 2 mM or 1 mM. Excess amount of sodium dithionite was added for the measurements of the reduced forms. 2,2-Dimethyl-2-silapentane-5-sulfonate sodium salt (DSS) was employed as an internal chemical shift reference.

Electrochemistry—All electrochemical measurements were done using a water-jacketed conical cell that allowed measurements to be made at controlled temperatures using volumes as small as 150 μl. An ALS electrochemical analyzer (model 611A) was used for all measurements. All solutions were purged with N_2 gas before use and blanketed with N_2 during the electrochemical determinations. The electrodes were derivatized with 100 mM of 3-mercaptopropionate. Poly-L-lysine was added to a final concentration of 25 μM just before the measurements. The formal potential of the LMWb5 were determined using Au electrodes pre-treated with 100 mM of 3-mercaptopropionate. The average of the cathodic and anodic peak potentials was taken as the formal potential. All potentials were measured versus a saturated calomel references (SCE) and are reported versus the standard hydrogen potential (NHE).

Protease Digestion of LMWb5—The digestion of oxidized LMWb5 (intact or DEPC-treated) sample (~50 μM) in 50 mM potassium-sodium phosphate (pH 7.0) buffer was started by addition of TPCK-treated trypsin (from bovine pancreas, Sigma Chemical Co., St. Louis, MO) solution (final concentration; 0.76 μM) and was continued at room temperature. The extent of the digestion was checked with mass spectrometric analysis with an appropriate interval.

MALDI-TOF Mass Spectrometry—Mass spectrometric analyses were carried out on a Voyager-DE Pro mass spectrometer (Applied Biosystems) using a 20 kV accelerating voltage. The mass spectra were acquired by adding the individual spectrum from 256 laser shots. For protein analysis the spectrometer was run in a linear mode and for peptide analysis in a reflector mode. The LMWb5 protein solutions were diluted 1:9 (v/v) with a matrix solution, 3,5-dimethoxy-4-hydroxycinnamic acid (Aldrich, Gillingham, England), 50 mg/ml in 30% acetonitrile in 0.3% TFA. The digested peptide solutions from LMWb5 were diluted 1:9 (v/v) with a matrix solution, α-cyano-4-hydroxycinnamic acid (Aldrich, Gillingham, England), 50 mg/ml in 50% acetonitrile in 0.3% TFA. The mixtures (typically, 1.0 μl) were deposited on the sample plate and allowed to air-dry before the analysis. Insulin (bovine, 5,733.69 Da) and apomyoglobin (horse, 16,951.56 Da) were used as external standards for the protein analysis.

The positions of the protease cleavage sites and probable modification sites with DEPC in the LMWb5 amino acid sequence were identified using the program GPMAW (v 6.1) (Lighthouse Data, Odense M, Denmark), considering other possible side reactions (Lys, Cys, Arg, Tyr, and Ser) (*11*). The molecular masses of all polypeptides measured matched the theoretical ones obtained from the human cytochrome b_5 amino acid sequences (Table 1) within an accuracy of 0.1% or better.

NH_2-Terminal Amino Acid Sequencing of LMWb5—NH_2-terminal amino acid sequencing of LMWb5 was conducted as follows. Purified LMWb5 was further separated on SDS-PAGE followed by an electro-blotting onto a PVDF membrane (Immobilon PSQ, Millipore). The Ponceau S–stained band corresponding to LMWb5 on the PVDF membrane was cut and was directly analyzed with an ABI protein sequencer (Model 492; Applied Biosystems) up to 10 cycles.

Table 1. **Amino acid sequences of theoretical tryptic peptides of LMWb5 (human).**

From–To	MH^+	Sequence
1–10	1,108.21	MAEQSDEAVK
11–19	1,187.33	YYTLEEIQK
20–24	622.66	HNHSK
25–33	1,135.35	STWLILHHK
34–39	738.86	VYDLTK
40–52	1,512.66	FLEE**H**PGGEEVLR
53–73	2,207.19	EQAGGDATENFEDVG**H**STDAR
74–77	494.59	EMSK
78–91	1,638.86	TFIIGELHPDDRPK
92–99	912.07	LNKPPETL

[a]Seven His residues are underlined. [b]Heme axial ligands (His 44 and His68) are indicated in boldface type.

RESULTS

Properties of Soluble Domain of Human Cytochrome b_5 *(LMWb5)*—The purified LMWb5 showed characteristic visible absorption spectra for oxidized and reduced forms of cytochrome b_5 with absorption peaks at 413 nm for oxidized form and at 556, 526, and 423 nm for reduced form (spectra not shown). The EPR spectrum of oxidized LMWb5 measured at 15K showed $g_z = 3.03$, $g_y = 2.20$, and $g_x = 1.41$ (Fig. 1A; trace a), very close to those reported in literature (*17*). It must be noted that there was no high-spin signals around $g \sim 6$ nor the signals from adventitiously bound non-heme iron at $g = 4.3$ in the spectra measured at 15 K and 8 K (Fig. 1, A and B; traces a) (*17*). The Au electrode pre-treated with polylysine gave quasi-reversible voltammetric responses for the LMWb5 solution (cyclic voltammogram, not shown) and the midpoint potential was estimated as –21 mV (*vs.* NHE), close to the value for bovine liver cytochrome b_5 (–10 mV) (*18*).

Purified LMWb5 showed a single protein-staining band (CBB-250 staining) upon SDS-PAGE (12% gel) analysis with an apparent molecular size of 16.5 kDa. This value was, however, much larger than the expected value for the soluble domain (1–99 aa; with an estimated value of 11,358.58 Da). To clarify the biochemical nature of the LMWb5, we conducted MALDI-TOF-MS analyses. Untreated LMWb5 sample showed a single peak with 11,263.9 m/z corresponding to a mono-protonated form. A doubly-protonated form showed a weak peak with 5,560.3 m/z. This result suggested that a post-translational modification had occurred in LMWb5. The NH_2-terminal amino acid sequencing (10 cycles) of the intact LMWb5 showed a sequence of AEQSDEAVKY, corresponding to the sequence of 2–11 (Table 1). MALDI-TOF-MS analyses on the tryptic peptides of LMWb5 (data not shown) also suggested that the Met residue at the initiation site was removed post-translationally. We concluded that LMWb5 is a form with the sequence corresponding to 2–99 aa of human cytochrome b_5 (theoretical molecular weight with 11,254.39 Da).

Reaction of LMWb5 with DEPC—Reaction of DEPC with oxidized form of LMWb5 was examined spectrophotometrically in the ultraviolet and visible regions with a difference spectrum mode. At a lower concentration of DEPC [LMWb5 (30 μM):DEPC (0.5 mM) = 1:16; molar ratio],

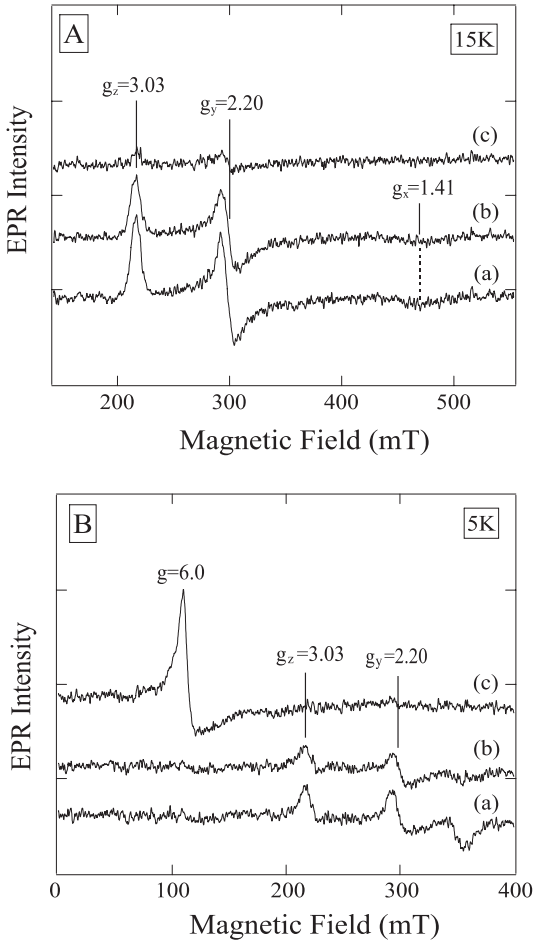

Fig. 1. **X-band EPR spectra of oxidized LMWb5 and effects of the DEPC-treatments on the spectra measured at 15 K (A) and 5 K (B).** In each panel, control (trace a), DEPC-treated at the lower concentration (0.5 mM) (trace b), and DEPC-reduced at the higher concentration (3.0 mM) (trace c) LMWb5 are shown. Other conditions are described in the text.

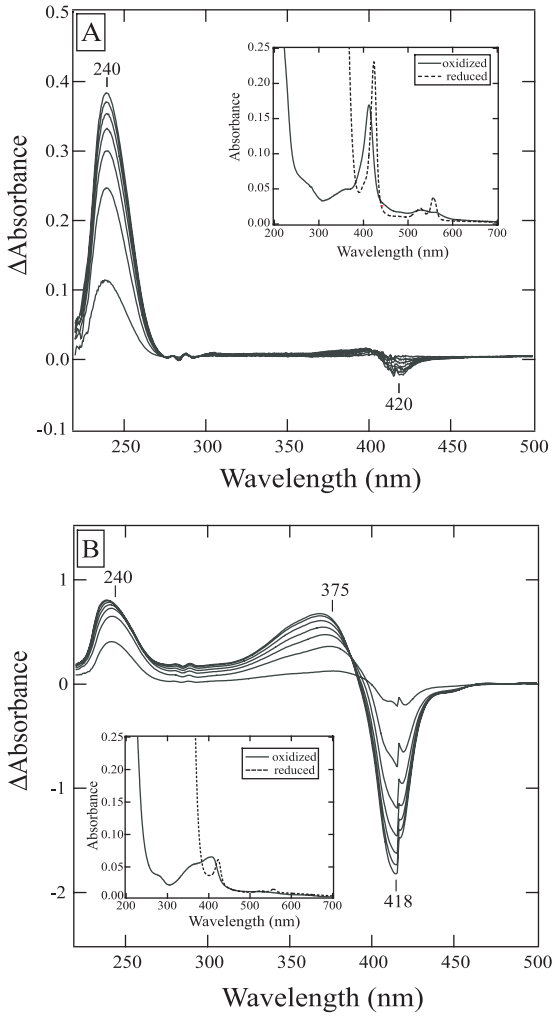

Fig. 2. **Changes in difference UV spectra upon the DEPC-treatment of oxidized LMWb5.** Optical quartz cells (light path, 1.0 cm) containing 1.0 ml each of oxidized LMWb5 [11.2 μM in 50 mM potassium-phosphate buffer (pH 6.5)] were placed in sample and reference cell holders of a spectrophotometer. The base line was recorded before the reaction started. DEPC (16.7 μl of 30 mM solution in dried MeOH) and an equal amount of MeOH were added to the sample [final DEPC concentration, 0.5 mM (panel A) or 3.0 mM (panel B)] and the reference cells, respectively. The spectral change was recorded in a 2.5 min-interval in the region from 500 to 220 nm (taking 1 min and 40 s for each scan) at room temperature. Insets in each panel showed visible absorption spectra of the DEPC-treated LMWb5 in oxidized and dithionite ($Na_2S_2O_4$)-reduced states. Other conditions were described in the text.

there was a time-dependent and steady increase in absorbance at 240 nm (Fig. 2A), indicating the progression of *N*-carbethoxylation of imidazole groups. From the increase in the absorbance, we estimated the number of the modified His residues as 4.5 per molecule using the extinction coefficient of 3.2 mM^{-1} cm^{-1} at 240 nm (*11*). In the visible region, there was a slight decrease in the absorbance around 420 nm (ΔA_{420} = ∼ –0.035); however, the degree of the change was very small compared to the changes at 240 nm if one considers the strong intensity of the Soret band. When we checked the absorbance spectra of the DEPC-treated LMWb5 in both oxidized and reduced states after removal of unreacted reagent, the spectra were indistinguishable from that of the untreated sample. On the other hand, when LMWb5 was treated at a higher concentration of DEPC [LMWb5 (30 μM):DEPC (3.0 mM) = 1:100 molar ratio], the increase of the absorbance at 240 nm was very rapid and significant, approaching to an estimated DEPC-modification number of 8.3 per molecule (corresponding to the level where all the His residues including the two heme-coordinating His residues were modified) (Fig. 2B). The absorbance change in the Soret band region was also significant; as the reaction proceeded, a clear derivative-shaped spectral change (minimum at 418 nm and maximum at 375 nm) developed (ΔA_{420} = ∼ –1.2) indicating the conversion of a low-spin to a high-spin heme species. The absorption spectra of the DEPC-treated (at a higher concentration with 1:100) LMWb5 in oxidized and reduced states after the removal of the unreacted reagent with gel-filtration were so much different from those of the untreated sample or the sample treated at a lower concentration of DEPC (Fig. 2A, inset). In the absorption spectrum of the oxidized form, intensity of the Soret band decreased dramatically and a shoulder

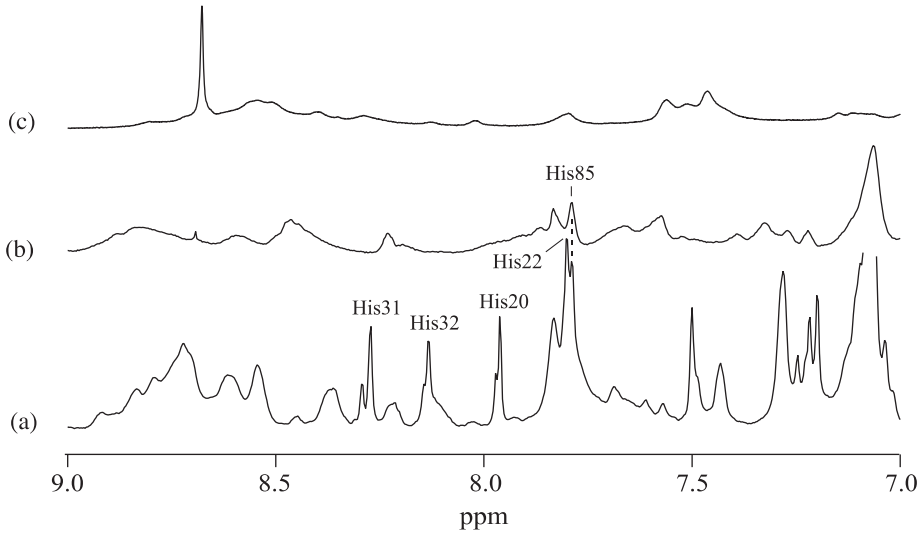

Fig. 3. **Effect of DEPC modification on the proton NMR spectrum of oxidized LMWb5 in the aromatic region.** LMWb5 was treated with DEPC, and the proton NMR spectra were obtained at pD 7.4 and 24°C as described under Materials and Methods. (Trace a), untreated native form; (trace b), DEPC-treated at a lower concentration; (trace c), DEPC-treated at higher concentration.

band around 360 nm increased in its intensity (Fig. 2B, inset). In the reduced form, intensity of the Soret band decreased significantly; less than 20% of the original intensity of the six-coordinated species remained as judged by the intensities of the Soret and α-bands (Fig. 2B, inset). These observations indicated that a significant part of the heme moiety became unstable after the treatment with a higher concentration (1:100) of DEPC, probably by a rupture of at least one Fe^{3+}-His coordination bond. Subsequently, a significant release of the heme prosthetic group from the protein moiety might occur (*12, 13*).

EPR Spectral Changes of LMWb5 upon the DEPC-Treatment—Effects of the DEPC-treatments on the heme moiety of LMWb5 were examined by EPR spectroscopy. Upon the treatment at a lower concentration of DEPC (1:16), the spectrum did not show any appreciable changes in both at 15 K and 8 K (Fig. 1, A and B; traces b). However, upon the treatment at a higher concentration of DEPC (1:100), the situation changed drastically. In the spectrum measured at 15 K, there was a trace amount of the native low-spin signals remaining at g_z = 3.03, g_y = 2.02, and g_x = 1.41 (Fig. 1A, trace c) (*19, 20, 17*). In the spectrum measured at 8 K, a strong g = 6.0 high-spin signal dominated and there was no low-spin signals (Fig. 1B, trace c). These observations suggested that the treatment with DEPC at a lower concentration (1:16) did not cause any appreciable influence on the heme moiety; but the treatment at a higher concentration (1:100) caused a rupture of at least one of the two Fe^{3+}-His coordination bonds. These results were fully consistent with the results obtained from visible and ultraviolet absorption spectra.

NMR Spectroscopic eExamination of the Effects of DEPC-Treatment—The hydrophilic domain of human cytochrome b_5 (LMWb5) contains total of 7 His residues (His20, His22, His31, His32, His44, His68, and His85)[2] including two heme-coordinating His residues (His44 and His68). To clarify the modification level of each His residue, we conducted ^{1}H-NMR spectroscopic measurements both in the oxidized (for the non-coordinating His residues and His44) and the reduced (for His68) forms. The ^{1}H-NMR spectra for the aromatic region of the LMWb5 sample pretreated with DEPC at a lower concentration (1:16) already showed a significant modification (Fig. 3, trace b), compared to those of the untreated sample (Fig. 3, trace a). The $C_{\varepsilon 1}$ protons of non-coordinating His residues [His20 (7.96 ppm), His22 (7.80 ppm), His31 (8.27 ppm), and His32 (8.13 ppm)] and the $C_{\delta 2}$ proton of His22 (7.50 ppm) completely disappeared and only the $C_{\varepsilon 1}$ proton of His85 (7.79 ppm) remained in the spectrum (the assignments were made based on Ref. *21*). This His85 is known as a residue with a low reactivity towards DEPC (*21*). On the other hand, intensities of the $C_{\delta 2}$ proton of His44 (–13.5 ppm; for the oxidized form) (*22*) and $C_{\varepsilon 1}$ and $C_{\delta 2}$ protons of His68 (0.77 and 0.35 ppm, respectively; for the reduced form) (*23, 24*) did not show appreciable changes upon the DEPC treatment at a lower concentration (spectra not shown), although the peaks showed some broadenings and slight chemical shifts. Upon treatment with a higher concentration of DEPC (1:100), all these proton signals disappeared completely (Fig. 3, trace c). These observations indicated that the modification sites with a lower DEPC concentration (1:16) were restricted only for the non-coordinating His residues; while with the treatment at a higher concentration of DEPC (1:100), the heme-coordinating His residues were also modified.

MALDI-TOF-MS Spectrometric Analyses of the DEPC-Treated LMWb5—To evaluate the histidyl modification sites and other possible modification sites with DEPC, we conducted MALDI-TOF-MS analyses on the tryptic peptides of LMWb5. The modification of a His residue(s) with DEPC could be detected by a mass increment of 72 m/z (or its multiples) of the untreated tryptic peptides (Table 1) due to a mono-substituted carbethoxy group on an imidazole ring or other possible reactive sites (*9, 25–27*).

The MALDI-TOF-MS spectra of the tryptic peptides obtained from the DEPC-treated LMWb5 (where LMWb5

[2] Numbering of amino acid residues in the present study is different from the crystallographic numbering. The seven His residues, His20, His22, His31, His32, His44, His68, and His85, correspond to His15, His17, His26, His27, His39, His63, and His80, respectively, of the crystallographic data for bovine cytochrome b_5 (Protein Data Bank, 1CYO).

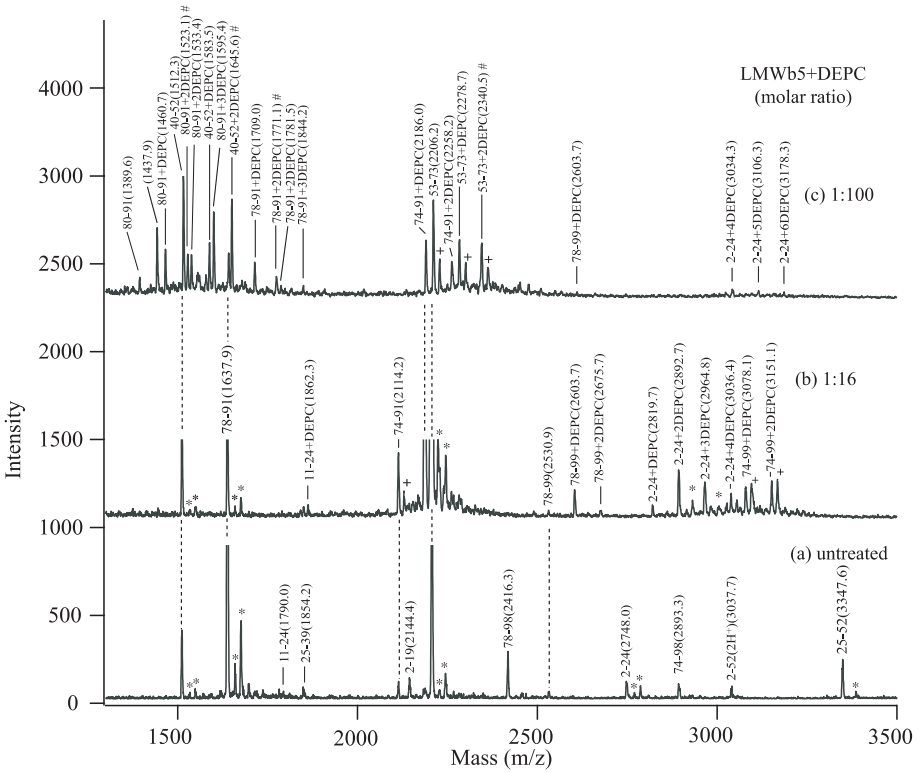

Fig. 4. **MALDI-TOF mass spectra of tryptic digests obtained from control (untreated) LMWb5 (a) and from LMWb5 pretreated with DEPC at the lower concentration (1:16) (b) and at the higher concentration (1:100) (c).** Tryptic digests were obtained as described in the text. A mixture of the polypeptides was directly analyzed with MALDI-TOF mass spectrometry. Other conditions are described in the text. The number for each peak indicates the assignment of each polypeptide by numbers of amino acid residues (from–to) in trace (a). The polypeptides containing carbethoxy group in trace (b) and (c) are shown as "from–to" and "+DEPC," "+2DEPC," and "+3DEPC," indicating the introduction of and its number of carbethoxy group into the polypeptide. The number in the parenthesis indicates the observed mass value (m/z) for each peak. The peptides having a ring-opened derivative are indicated by # at the most upper part of the corresponding peak. Peaks indicated by an asterisk are due to $[M+Na^+]$ and $[M+K^+]$ species. Peaks indicated by a + are due to oxidation (most likely the oxidation of Met75) or hydroxylation (+16.0 m/z).

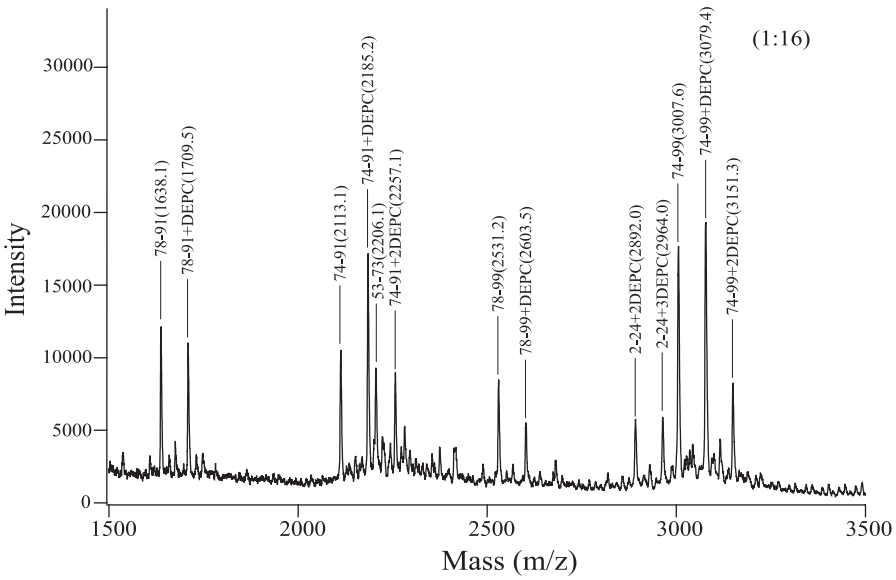

Fig. 5. **A part of the MALDI-TOF mass spectrum of tryptic digests obtained from LMWb5 treated with a lower concentration of DEPC.** Tryptic digests were obtained from LMWb5 treated with a lower concentration of DEPC (1:16) as described in the text. A mixture of the peptides, but in a digestion stage different from that of Fig. 4, was directly analyzed with MALDI-TOF mass spectrometry. Other conditions were the same as in Fig. 4.

was pretreated with DEPC in a 1:16 ratio and the resulting sample contained about 4.5 *N*-carbethoxy groups on its His residues) were characterized as followings (Fig. 4, traces a and b). (i) There was no *N*-carbethoxylation at the axial His residues (His44 and His68). (ii) Of the five non-axial His residues, the four reactive His residues (His20, His22, His31, and His32) showed an almost complete modification (mono-*N*-carbethoxylation) as indicated by the appearance of peptides [2–24+2DEPC (2,892.7 m/z); 2–24+3DEPC (2,964.8 m/z); 11–24+DEPC (1,860.9 m/z); 11–24+2DEPC (1,932.9 m/z); 25–33+3DEPC (1,350.35 m/z) (not shown in Fig. 4 for the last two peaks)] without any traces of unmodified peptides. (iii) One remaining non-axial His residue (His85) showed a lower reactivity toward DEPC than other four His residues as indicated by the appearance of several pairs of peptides [unmodified peptides 74–99 (3,007.6 m/z), 78–99 (2,530.2 m/z), 74–91 (2,113.1 m/z), 78–91 (1,638.1 m/z), and their mono-*N*-carbethoxylated peptides] (Fig. 5). (iv) Other than these His residues, several Lys (or Ser) residues were also modified partially as

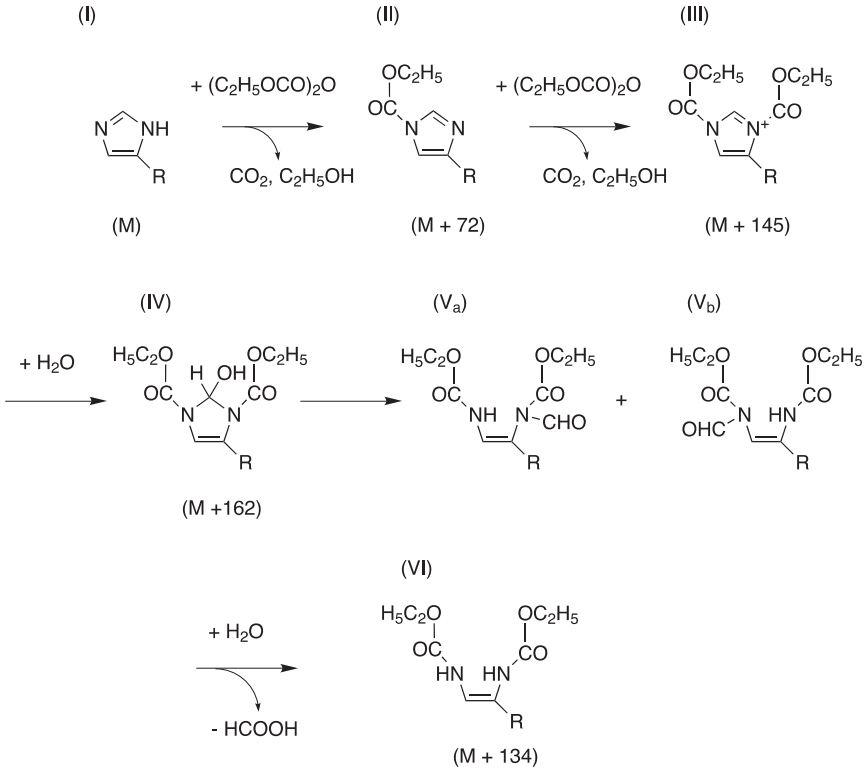

Fig. 6. **Reaction pathway of a hisitidine imidazole group with DEPC.** The imidazole group of the unmodified protein (**I**) and its mono-*N*-carbethoxylated (**II**) and bis-*N*-carbethoxylated products (**III**) after the DEPC-treatment are shown. The bis-*N*-carbethoxylated product (**III**) is, then, hydrated (**IV**), and is further converted to ring-opened derivatives ($\mathbf{V}_a$ and $\mathbf{V}_b$). The ring-opened derivatives further decompose slowly to bis-*N*-carbethoxylated, deformylated derivatives (**VI**) by hydrolysis. These ring-opened derivatives give stronger absorbance at 240 nm. The mass increments (in Da) caused by the carbethoxylation and by the subsequent hydrolysis are indicated in parenthesis.

indicated by the appearance of di-carbethoxylated or tri-carbethoxylated peptides with weak intensities [for Lys77, 74–99+2DEPC (3,151.3 *m/z*), 74–91+2DEPC (2,257.1 *m/z*) (Fig. 5); for Lys19, 2–24+3DEPC (2,964.0 *m/z*); for Ser25, 25–33+3DEPC (1,350.35 *m/z*); for Ser5, 2–10+DEPC (1,050.7 *m/z*) (not shown in Figs. 4 and 5 for the last two peaks)].

A MALDI-TOF-MS spectrum of the tryptic peptides obtained from the LMWb5 pretreated with DEPC in a 1:100 ratio is shown in Fig. 4 (trace c). Under this higher DEPC concentration, all His residues were modified on the basis of the UV absorption spectra and the ^{1}H-NMR spectra, as shown in previous sections. The MALDI-TOF-MS spectra of this sample were characterized as followings (Fig. 4, trace c). (i) Both of the axial ligands (His44 and His68) were modified significantly as indicated by the presence of peptides 40–52+DEPC (1,583.5 *m/z*) and 53–73+DEPC (2,278.7 *m/z*). (ii) Appearance of the second peptides with an additional mass increment of 62 for the mono-carbethoxylated peptides (1,645.6 *m/z* for the peptide 40–52+DEPC and 2,340.5 *m/z* for the peptide 53–73+DEPC) suggested that bis-*N*-carbethoxylation occurred on each of the axial imidazole ring (*26, 27*). (iii) One non-axial His residue (His85) with a lower reactivity toward DEPC also showed a bis-*N*-carbethoxylation on its imidazole ring; *i.e.*, appearance of a second peptide with an additional mass increment of 62 for the mono-carbethoxylated peptides (1,523.1 *m/z* for the peptide 80–91+DEPC and 1,771.1 *m/z* for the peptide 78–91+DEPC). (iv) The mass increment of 62 could be explained as shown in Fig. 6 (*27, 28*). In short, the bis-*N*-carbethoxylated product was hydrated, and was further converted to ring-opened derivatives. The ring-opened derivatives were further decomposed slowly to bis-*N*-carbethoxylated, deformylated derivatives by hydrolysis. The formation of the bis-*N*-carbethoxylated product might be a major reason for the discrepancy between the estimated number of the modified His residues based on the UV-absorption at 240 nm and the actual number of His residues in LMWb5 (Table 1); in which mono-*N*-carbethoxylated derivative had a smaller absorbance than the bis-*N*-carbethoxylated derivatives or the subsequent ring-opened derivatives (*28, 11, 29*). This lead to the estimated value of 8.3 at a higher DEPC concentration, whereas the total number of His residues in LMWb5 were only 7. Assuming the number of the modified His residues at a lower DEPC concentration to be correct (this is a reasonable assumption, since the MALDI-TOF-MS data indicated that 4 His residues were fully mono-*N*-carbethoxylated, about a half of one His residue was mono-*N*-carbethoxylated, and there was no bis-*N*-carbethoxylated derivatives), we could obtain a molar extinction coefficient value of 3.2 mM^{-1} cm^{-1} at 240 nm, an identical value with Miles (*11*). Upon treatment with a higher DEPC concentration, we assumed that 4.48 imidazole groups of the five non-axial His residues were mono-*N*-carbethoyated and 0.32 residues were ring-opened structure *via* bis-*N*-carbethoxylation; whereas for the remaining two axial ligands, 0.46 residues were mono-*N*-carbethoxylated, 0.64 residues were ring-opened structure *via* bis-*N*-carbethoxylation (Table 2). These estimations lead to an extinction coefficient value of 11.2 mM^{-1} cm^{-1} at 240 nm for the ring-opened derivatives. This value is much higher than the value for the mono-*N*-carbethoxylated derivative and is about a half of the value obtained for the ring-opened imidazole derivatives (*28*).

Table 2. **Estimation of the mono- and bis-*N*-carbethoylated His residues in LMWb5 (human) upon treatment with a higher concentration of DEPC (2.0 mM).**

	Intact	Mono-*N*-carbethoxylated	Ring-opened bis-*N*-carbethoxylated
His44	0.43	0.20	0.37
His68	0.47	0.26	0.27
His80	0.20	0.48	0.32
His20	0	1.0	0
His22	0	1.0	0
His31	0	1.0	0
His32	0	1.0	0
Total	1.10	4.94	0.96

In the analysis, we assumed that all the bis-*N*-carbethoxylated His residues were converted to the ring-opened derivatives. Although the quantitative analysis using MALDI-TOF-MS data are not so reliable, we estimated the extent of carbethoxylation based on a comparison of relative band intensities of the triplets (intact, mono-*N*-carbethoxylated, and ring-opened bis-*N*-carbethoxylated derivatives) for the same length of peptides in the MALDI-TOF-MS spectrum. Such comparisons would be much more reliable than using an internal standard peptide.

DISCUSSION

Reactivity of Non-Axial and Axial His Residues in LMWb5 toward DEPC—DEPC is an electrophilic reagent that has been used to modify His residues of proteins in a relatively specific manner (*11*). The crystal structure of the soluble domain of bovine cytochrome b_5 (1CYO) (*30–32*) indicated that axial His residues (His39 and His63, corresponding to His44 and His68 of LMWb5) would not be available for the chemical modification at a lower concentration of reagents, such as DEPC. However, Konopka and Waskell showed that the treatment of rabbit and bovine cytochrome b_5 at higher concentrations of DEPC modified the axial His residues and displaced the heme prosthetic group (*12, 13*). Previous ^{1}H-NMR study on bovine cytochrome b_5 treated with DEPC showed that the non-axial His residues were modified sequentially with increasing DEPC concentration in the order His31 $\approx$ His32 > His20 $\geqslant$ His22 > His85 (*21*). Although no detailed analysis was made for the axial His residues, it was postulated that the reactivity of the two axial His residues (His44 and His68) were much lower than other non-axial His residues (*12*).

Our present study indicated as follows. (i) Upon treatment with a lower concentration of DEPC, five non-axial His residues (His31, His32, His20, His22, His85, in which the least modified residue being His85) of LMWb5 were easily modified; but remaining two axial His residues (His44 and His68) were not modified at all. (ii) Upon treatment with DEPC at a higher concentration, the two axial His residues were modified and subsequently the heme prosthetic group was displaced. (iii) During the reaction of the axial His residues with DEPC, bis-*N*-carbethoxylation of the imidazole ring might occur (Fig. 6), although the bis-*N*-carbethoxylated peptide (containing the derivatives either **IV**, $\mathbf{V}_a$, or $\mathbf{V}_b$) was not identified directly in our present MALDI-TOF-MS spectra. However, formation of the ring-opened derivatives ($\mathbf{V}_a$ and $\mathbf{V}_b$) followed by hydrolysis to produce the bis-*N*-carbethoxylated, deformylated derivatives (**VI**), identified in the present study, suggested unambiguously that the bis-*N*-carbethoxylation had occurred at the heme-coordinating imidazole rings (both His44 and His68). (iv) The least reactive non-axial His residue (His85) was also found to form bis-*N*-carbethoxylated, deformylated derivatives (**VI**), upon treatment with a higher DEPC concentration.

Mechanism of the DEPC Reactivity for His Residues in LMWb5—The neutral imidazole ring of a His residue can exist in two tautomeric forms: either the $N_{\varepsilon 2}$-H tautomer or the $N_{\delta 1}$-H tautomer (*33*). DEPC reacts with the deprotonated nitrogen atom of an imidazole ring according to the reaction scheme of Miles (*11*); *i.e.*, the reaction occurs by an initial attack of the electrophilic carbon of DEPC at the nitrogen without a hydrogen atom. The reactivity of an imidazole group with DEPC will be influenced by (i) the steric accessibility of the imidazole to the solvent, (ii) the hydrogen-bonding interactions with other amino acid residues, and (iii) the pK_a of the imidazole group. However, it must be noted that these factors will be mutually influenced.

One may be puzzled that non-axial His residues (His20, His22, His31, and His32) of LMWb5 did not show any formation of the ring-opened derivative upon treatment with DEPC at a higher concentration, despite of their initial higher reactivity towards DEPC. Such higher reactivity might be considered as due to the higher accessibility of their imidazole groups to the solvent. If so, this should lead to a higher probability to form a bis-*N*-carbethoxylated derivative, leading to the formation of ring-opened derivatives at these residues. However, it did not actually occur.

It was demonstrated previously that non-axial His residues form a mixture with approximately a 4:1 (or 7:3) preference for $N_{\varepsilon 2}$-H protonation over $N_{\delta 1}$-H protonation based on the analysis of free histidine (or N_α-acetylhistidine methylamide). This is due to the fact that $N_{\varepsilon 2}$ and $N_{\delta 1}$ atoms of the imidazole ring have distinct microscopic pK_a: the $N_{\delta 1}$ pK_a (=6.12) being more acidic than the $N_{\varepsilon 2}$ pK_a (=6.73) (*33, 34*). This would lead to a preferable carbethoxylation at the $N_{\delta 1}$ position for the non-axial His residues, if steric factors were not considered. Once such a mono-$N_{\delta 1}$-carbethoxylated derivative was formed, further carbethoxylation at $N_{\varepsilon 2}$ atom of the same ring will be depressed due to a still higher pK_a value at the $N_{\varepsilon 2}$ position (*33*). Therefore, only for the derivative in which the first *N*-carbethoxylation occurred at $N_{\varepsilon 2}$ atom, there will be a further $N_{\delta 1}$-carbethoxylation to take place on the same imidazole ring, resulting in the formation of the bis-*N*-carbethoxylated derivatives and the subsequent ring-opened derivatives (*11, 27, 28*).

The formation of the bis-*N*-carbethoxylated derivatives at non-axial His85 is exactly following this scenario. Although its solvent accessibility is rather high, the $N_{\delta 1}$ atom of His85 works as the hydrogen acceptor in a strong hydrogen bond with a nitrogen atom of the main-chain amide of Asp87 (*21, 35*). Therefore, the only nitrogen available to react with DEPC is the $N_{\varepsilon 2}$ atom but in a protonated form. This is the reason for the low reactivity of His85 toward DEPC as previously suggested (*21*). However, once the first *N*-carbethoxylation occurred at the $N_{\varepsilon 2}$ atom with a higher DEPC concentration, the subsequent $N_{\delta 1}$-carbethoxylation by breaking the strong hydrogen bond would take place leading to the formation

of the bis-*N*-carbethoxylated derivatives and the subsequent ring-opened derivatives.

For the two axial His residues (His44 and His68), a similar but distinct mechanism might be operative. Since the $N_{\varepsilon 2}$ atom of an imidazole ring coordinates to Fe^{3+} iron of the heme prosthetic group as found in cytochrome b_5 and many other heme-containing proteins, the $N_{\delta 1}$-H tautomer is stabilized for the axial His residues in hemoproteins. Presence of the hydrogen-bonding interaction (mediated by $N_{\delta 1}$-H) with surrounding amino acid residues strengthens further the $N_{\delta 1}$-H tautomer (*24*). Therefore, the primary reactive site of the axial His ligands with DEPC is expected to be as the $N_{\varepsilon 2}$ position, if enough concentrations of DEPC were provided to overcome the protective effect by the Fe^{3+}-$N_{\varepsilon 2}$ coordination bond. As expected, our present results showed that the displacement of the heme prosthetic group occurred upon the treatment with a higher concentration of DEPC, indicating a rupture of the Fe^{3+}-$N_{\varepsilon 2}$–bond by the *N*-carbethoxylation of the coordinating $N_{\varepsilon 2}$ atom, and the other $N_{\delta 1}$ atom in the same imidazole ring was also *N*-carbethoxylated concomitantly. Indeed, it was reported that the formation of a mono-$N_{\varepsilon 2}$-carbethoxylated derivative caused a lowering of pK_a value at the $N_{\delta 1}$ position (*33*). This effect (applicable for the axial His residues and His85) would cause a further promotion of the carbethoxylation at the $N_{\delta 1}$ position leading to the ring-opened derivatives.

Comparison of the DEPC Reactivity with Other Heme Axial His Ligands—At this moment, it might be very informative to compare the present results with those obtained for other hemoproteins having a bis-His coordination. Our recent study on a six-coordinated myoglobin mutant (VHA-Mb), in which triple mutations (H64V/V68H/H93A) were introduced in porcine myoglobin to adopt a six-coordinated heme prosthetic group, showed similar results with those obtained in the present study (Nakanishi *et al*., unpublished). VHA-Mb contains 6 non-axial His residues (His24, His36, His48, His81, His82, and His119) besides two axial His residues (His68 and His97)[3]. The non-axial His residues were easily modified with low concentrations of DEPC (0.02–1.0 mM) but the other two axial His residues showed no indication of the modification under the same conditions. However, once *N*-carbethoxylation occurred at the $N_{\varepsilon 2}$ position of one axial His (His97) with a higher concentration of DEPC (2.0–5.0 mM), as evidenced by a displacement of a heme prosthetic group from the protein moiety, it facilitated the second *N*-carbethoxylation to take place at the $N_{\delta 1}$ position of the same imidazole ring, leading to a bis-*N*-carbethoxylated derivative and further to a ring-opened derivative (Nakanishi *et al*., unpublished). The other axial His (His68) did not show any indication of *N*-carbethoxylation even at the highest DEPC concentration (5.0 mM). These results are consistent with the notion that His68 is located deeply inside of the protein moiety and its Fe^{3+}-$N_{\varepsilon 2}$ bond must be strong enough to withstand the attack from DEPC. On the other hand, His97 is expected as locating relatively closer to the protein surface (leading to the lowering of the shielding effect) and its elongated Fe^{3+}-$N_{\varepsilon 2}$ bond might be vulnerable to the attack from DEPC.

A more interesting comparison might be made with the results for cytochrome b_{561}. Cytochrome b_{561} contains two heme centers. One heme center locating on the intravesicular side of the molecule has two His axial ligands (His54 and His122) (*36*). However, these two His residues did not show any signs of *N*-carbethoxylation even after the treatment with a relatively higher DEPC concentration (3–5 mM) (*7, 9*), despite the indications as relatively surface-exposed (*36*). Therefore, it might be concluded that these two His residues each have a strong coordination bond to the heme iron and their protons at the $N_{\delta 1}$ position were well-stabilized, as found for other usual heme-containign proteins.

On the other hand, the other heme center on the cytosolic side of cytochrome b_{561} showed both a specific *N*-carbethoxylation of its coordinating histidyl imidazole ligands (His88 and His161) and a significant loss of the fast electron acceptance ability from AsA upon the treatment with a lower concentration of DEPC (0.5 mM) (*7–9*). Although small but distinct spectral changes[4] occurred upon the DEPC treatment, there was no release of heme *b* prosthetic group from the protein moiety (*9*). Since DEPC specifically attacks the deprotonated nitrogen atom of an imidazole ring as described above, it is indicative that the non-coordinating nitrogen atom (most likely $N_{\delta 1}$) of the coordinating imidazole group at the cytosolic heme center is deprotonated at physiological pH and, therefore, might be specifically *N*-carbethoxylated. However, as described in the previous section, the $N_{\delta 1}$ atom of the heme axial His residues are generally protonated and participates in a hydrogen-bond network with nearby amino acid residues as found for bovine cytochrome b_5 (*24*). Therefore, there must be a specific mechanism in operation to maintain the deprotonated state of the $N_{\delta 1}$ atom of axial His

[3] The heme-coordination of VHA-Mb in ferrous state is found to have a bis-His (His68/His97) structure based on visible absorption spectra, resonance Raman spectra, and cyanide-binding affinity (*3*). On the other hand, VHA-Mb in ferric state is reported to have a His68/hydroxide structure based on resonance Raman profiles and visible absorption spectra (*3*). However, cyanide-binding affinity of VHA-Mb in ferric state (K_d = 2.04 mM) was much lower than those of WT-Mb (1.87 μM), VHAF-Mb (5.85 μM), or VHGF-Mb (5.65 μM), where a water or hydroxide ion was expected to bind to the ferric heme as a distal ligand (*3*) and was comparable to that of the VH double mutant (8.51 mM), in which the bis-His coordination structure was verified by X-ray crystallography (*4*). Further, the pH titration of VHA-Mb in ferric state showed a very similar profile in spectral changes with that of VH double mutant (*3*). These observations suggested that the distal hydroxide ligand of VHA-Mb in ferric state might be strongly stabilized by a hydrogen bond with distal His97 residue to prevent the ligand exchange with cyanide ion or, more likely, that the His97 imidazole itself might coordinate directly to the ferric heme.

[4] Such relatively minor perturbation in electronic absorption spectra might be comparable to those found for H93G proximal cavity mutant of myoglobin, where the proximal His has been replaced with Gly, creating a cavity which can be occupied by a variety of exogenous ligands (*5, 6*). Exogenously added imidazole could coordinate heme iron of H93G myoglobin as the proximal ligand, showing almost identical spectroscopic characteristics with those of wild-type myoglobin, despite of a significant rotation (~45°) of imidazole plane and a decreased distance between the heme and the proximal imidazole (*5*). Further, when imidazole was replaced with other small organic ligands, such as pyridine and methyl-substituted imidazoles, relatively minor changes in absorption spectra occurred (*6*).

residues at the cytosolic heme center of cytochrome b_{561}. As one possible mechanism, presence of some positively charged residue(s) at the immediate vicinity of the $N_{\delta1}$ atom might cause a significant decrease in a microscopic pK_a value of the $N_{\delta1}$ atom. Indeed, we have postulated the presence of an AsA-binding site comprised with well-conserved Lys and Arg residues near the cytosolic heme center (*7, 37*). It must be noted, however, that both LMWb5 and VHA-Mb have an essentially globular domain but cytochrome b_{561} has hemes being inserted between hydrophobic transmembrane helices. Therefore, we may have to consider an additional possibility that such different environments of the His axial ligands by definition may cause some difference in the reactivity with DEPC.

In conclusion, we found that the axial His ligands of LMWb5 were protected from the modification with DEPC by a limited steric exposure of the axial imidazole group to the solvent, by the Fe-$N_{\varepsilon2}$ coordination bond, and by the protonation of $N_{\delta1}$ atom forming a hydrogen-bond with its immediate surroundings. However, once the *N*-carbethoxylation at the $N_{\varepsilon2}$ position occurred, as evidenced by a displacement of the heme prosthetic group, it facilitates the second carbethoxylation to take place at the $N_{\delta1}$ position of the same imidazole ring, leading to the bis-*N*-carbethoxylated derivative and, further, to the ring-opened derivatives. Present results suggested that the use of DEPC for the MALDI-TOF-MS analysis might provide a unique method to characterize the protonation state of His residues and the strength of their hydrogen bondings at the active site of enzymes.

REFERENCES

1. Iverson, T.M., Arciero, D.M., Hsu, B.T., Logan, M.S.P., Hooper, A.B., and Rees, D.C. (1998) Heme packing motifs revealed by the crystal structure of the tetra-haem cytochrome c554 from *Nitrosomonas europaea*. *Nat. Struct. Biol.* **5**, 1005–1012
2. Rotsaert, F.A.J., Hallberg, B.M., de Vries, S., Moenne-Loccoz, P., Divne, C., Benganathan, V., and Goold, M.H. (2003) Biophysical and structural analysis of a novel heme *b* iron ligation in the flavocytochrome cellobiose dehydrogenase. *J. Biol. Chem.* **278**, 33224–33231
3. Uno, T., Sakamoto, R., Tomisugi, Y., Ishikawa, Y., and Wilkinson, A.J. (2003) Inversion of axial coordination in myoglobin to create a "proximal" ligand binding pocket. *Biochemistry* **42**, 10191–10199
4. Dou, Y., Admiraal, S.J., Ikeda-Saito, M., Krzywda, S., Wilkinson, A.J., Li, T., Olson, J.S., Prince, R.C., Pickering, I.J., and George, G.N. (1995) Alteration of axial coordination by protein engineering in myoglobin Bisimidazole ligation in the His^{64}→Val/Val^{68}→His double mutant. *J. Biol. Chem.* **270**, 15993–16001
5. Barrick, D. (1994) Replacement of the proximal ligand of sperm whale myoglobin with free imidazole in the mutant His-93→Gly. *Biochemistry* **33**, 6546–6554
6. DePillis, G.D., Decatur, S.M., Barrick, D., and Boxer, S.G. (1994) Functional cavities in proteins: A general method for proximal ligand substitutions in myoglobin. *J. Am. Chem. Soc.* **116**, 6981–6982
7. Takeuchi, F., Kobayashi, K., Tagawa, S., and Tsubaki, M. (2001) Ascorbate inhibits the carbethoxylation of two histidyl and one tyrosyl residues indispensable for the transmembrane electron transfer reaction of cytochrome b_{561}. *Biochemistry* **40**, 4067–4076
8. Takigami, T., Takeuchi, F., Nakagawa, M., Hase, T. and Tsubaki, M. (2003) Stopped-flow analyses on the reaction of ascorbate with cytochrome *b*561 purified from bovine chromaffin vesicle membranes. *Biochemistry* **42**, 8110–8118
9. Tsubaki, M., Kobayashi, K., Ichise, T., Takeuchi, F., and Tagawa, S. (2000) Diethylpyrocarbonate-modification abolishes fast electron accepting ability of cytochrome b_{561} from ascorbate but does not influence on electron donation to monodehydroascorbate radical: Distinct roles of two heme centers for electron transfer across the chromaffin vesicle membranes. *Biochemistry* **39**, 3276–3284
10. Tsubaki, M., Nakayama, M., Okuyama, E., Ichikawa, Y., and Hori, H. (1997) Existence of two heme B centers in cytochrome b_{561} from bovine adrenal chromaffin vesicles as revealed by a new purification procedure and EPR spectroscopy. *J. Biol. Chem.* **272**, 23206–23210
11. Miles, E.W. (1977) Modification of histidyl residues in proteins by diethylpyrocarbonate. *Methods Enzymol.* **47**, 431–442
12. Konopka, K. and Waskell, L. (1988) Chemical modification of cytochrome b_5, cytochrome *c* and myoglobin with diethylpyrocarbonate. *Biochim. Biophys. Acta* **954**, 189–200
13. Konopka, K. and Waskell, L. (1988) Modification of trypsin-solubilized cytochrome b_5, apocytochrome b_5, and liposome-bound cytochrome b_5 by diethylpyrocarbonate. *Arch. Biochem. Biophys.* **261**, 55–63
14. Cooper, M.T. and Porter, T.D. (2001) Cytochrome b_5 coexpression increases the CYP2E1-dependent mutagenicity of dialkylnitrosamines in methyltransferase-deficient strains of *Salmonella typhimurium*. *Mutat. Res.* **484**, 61–68
15. Mokashi, V., Li, L., and Porter, T.D. (2003) Cytochrome b_5 reductase and cytochrome b_5 support the CYP2E1-mediated activation of nitrosamines in a recombinant Ames test. *Arch. Biochem. Biophys.* **412**, 147–152
16. Muchmore, D.C., McIntosh, L.P., Russel, C.B., Anderson, D.E., and Dahlquist, F.W. (1989) Expression and nitrogen-15 labeling of proteins for proton and nitrogen-15 nuclear magnetic resonance. *Methods Enzymol.* **177**, 44–73
17. Sarma, S., DiGate, R.J., Goodin, D.B., Miller, C.J., and Guiles, R.D. (1997) Effect of axial ligand plane reorientation on electronic and electrochemical properties observed in the A67V mutant of rat cytochrome b_5. *Biochemistry* **36**, 5658–5668
18. Xue, L.-L., Wang, Y.-H., Xie, Y., Yao, P., Wang, W.-H., Qian, W., and Huang, Z.-X. (1999) Effect of mutation at valine 61 on the three-dimensional structure, stability, and redox potential of cytochrome b_5. *Biochemistry* **38**, 11961–11972
19. Guzov, V.M., Houston, H.L., Murataliev, M.B., Walker, F.A., and Feyereisen, R. (1996) Molecular cloning, overexpression in *Escherichia coli*, structural and functional characterization of house fly cytochrome b_5. *J. Biol. Chem.* **271**, 26637–26645
20. Ikeda, M., Iizuka, T., Takao, H., and Hagihara, B. (1974) Studies on the heme environment of oxidized cytochrome b_5. *Biochim. Biophys. Acta* **336**, 15–24
21. Altman, J., Lipka, J.J., Kuntz, I., and Waskell, L. (1989) Identification by proton nuclear magnetic resonance of the histidines in cytochrome b_5 modified by diethyl pyrocarbonate. *Biochemistry* **28**, 7516–7523
22. McLachlan, S.J., La Mar, G.N., and Lee, K.-B. (1988) One- and two-dimensional nuclear Overhauser effect studies of the electronic/molecular structure of the heme cavity of ferricytochrome b_5. *Biochim. Biophys. Acta* **957**, 430–445
23. Guiles, R.D., Altman, J., Kuntz, I.D., and Waskell, L. (1990) Structural studies of cytochrome b_5: Complete sequence-specific resonance assignments for the trypsin-solubilized microsomal ferrocytochrome b_5 obtained from pig and calf. *Biochemistry* **29**, 1276–1289
24. Lee, K.-B., McLachlan, S.J., and La Mar, G.N. (1994) Hydrogen isotope effects on the proton magnetic resonance spectrum of bovine ferricytochrome b_5: Axial hydrogen bonding involving the axial His-39 imidazole ligand. *Biochim. Biophys. Acta* **1208**, 22–30

25. Dage, J.L., Sun, H., and Halsall, H.B. (1998) Determination of diethylpyrocarbonate-modified amino acid residues in α_1-acid glycoprotein by high-performance liquid chromatography electrospray ionization-mass spectrometry and matrix-assisted laser desorption/ionization time-of-flight-mass spectrometry. *Anal. Biochem.* **257**, 176–185
26. Glocker, M.O., Kalkum, M., Yamamoto, R., and Schreurs, J. (1996) Selective biochemical modification of functional residues in recombinant human macrophage colony-stimulating factor β (rhM-CSF β): Identification by mass spectrometry. *Biochemistry* **35**, 14265–14633
27. Kalkum, M., Przybylski, M., and Glocker, M.O. (1998) Structure characterization of functional histidine residues and carbethoylated derivatives in peptides and proteins by mass spectrometry. *Bioconju. Chem.* **9**, 226–235
28. Loosemore, M.J. and Pratt, R.F. (1976) The irreversible cleavage of histidine residues by diethylpyrocarbonate (ethoxyformic anhydride). *FEBS Lett.* **72**, 155–158
29. Roosemont, J.L. (1978) Reaction of histidine residues in proteins with diethylpyrocarbonate: Differential molar absorptivities and reactivities. *Anal. Biochem.* **88**, 314–320
30. Argos, P. and Mathews, F.S. (1975) The structure of ferrocytochrome b5 at 2.8Å resolution. *J. Biol. Chem.* **250**, 747–751
31. Durley, R.C. and Mathews, F.S. (1996) Refinement and structural analysis of bovine cytochrome b_5 at 1.5 Å resolution. *Acta Crystallogr D Biol Crystallogr* **52**, 65–76
32. Mathews, F.S., Levine, M., and Argos, P. (1972) Three-dimensional Fourier synthesis of calf cytochrome b5 at 2.8 Å resolution. *J. Mol. Biol.* **64**, 449–464
33. Tanokura, M. (1983) ^{1}H-NMR study on the tautomerism of the imidazole ring of histidine residues I. Microscopic pK values and molar ratios of tautomers in histidine-containing peptides. *Biochim. Biophys. Acta* **742**, 576–585
34. Wolff, N., Deniau, C., Létoffé, S., Simenel, C., Kumar, V., Stojiljkovic, I., Wandersman, C., Delepierre, M., and Lecroisey, A. (2002) Histidine pK_a shifts and changes of tautomeric states induced by the binding of gallium-protoporphyrin IX in the hemophore $HasA_{sm}$. *Protein Science* **11**, 757–765
35. Mathews, F.S., Czerwinski, E.W., and Argos, P. (1979) The X-ray crystallographic structure of calf liver cytochrome b_5 in *The Porphyrins* (Dolphin, D., ed.) pp. 107–147, Academic Press, London
36. Okuyama, E., Yamamoto, R., Ichikawa, Y., and Tsubaki, M. (1998) Structural basis for the electron transfer across the chromaffin vesicle membranes catalyzed by cytochrome b_{561}: Analyses of cDNA nucleotide sequences and visible absorption spectra. *Biochim. Biophys. Acta* **1383**, 269–278
37. Tsubaki, M., Takeuchi, F., and Nakanishi, N. (2005) Cytochrome b561 protein family: Expanding roles and versatile transmembrane electron transfer abilities as predicted by a new classification system and protein sequence motif analyses. *Biochim. Biophys. Acta* **1753**, 174–190